

# Computational and experimental investigations of one-step conversion of poly(carbonate)s into value-added poly(aryl ether sulfone)s

Gavin O. Jones<sup>a,1</sup>, Alexander Yuen<sup>a</sup>, Rudy J. Wojtecki<sup>a</sup>, James L. Hedrick<sup>a</sup>, and Jeannette M. García<sup>a,1</sup>

<sup>a</sup>IBM Research–Almaden, San Jose, CA 95120

Edited by Miguel A. Garcia-Garibay, University of California, Los Angeles, CA, and accepted by Editorial Board Member R. D. Levine May 19, 2016 (received for review January 18, 2016)

It is estimated that ~2.7 million tons poly(carbonate)s (PCs) are produced annually worldwide. In 2008, retailers pulled products from store shelves after reports of bisphenol A (BPA) leaching from baby bottles, reusable drink bottles, and other retail products. Since PCs are not typically recycled, a need for the repurposing of the PC waste has arisen. We report the one-step synthesis of poly(aryl ether sulfone)s (PSUs) from the depolymerization of PCs and in situ polycondensation with bis(aryl fluorides) in the presence of carbonate salts. PSUs are high-performance engineering thermoplastics that are commonly used for reverse osmosis and water purification membranes, medical equipment, as well as high temperature applications. PSUs generated through this cascade approach were isolated in high purity and yield with the expected thermal properties and represent a procedure for direct conversion of one class of polymer to another in a single step. Computational investigations performed with density functional theory predict that the carbonate salt plays two important catalytic roles in this reaction: it decomposes the PCs by nucleophilic attack, and in the subsequent polyether formation process, it promotes the reaction of phenolate dimers formed in situ with the aryl fluorides present. We envision repurposing poly(BPA carbonate) for the production of value-added polymers.

polycondensation | recycling | polymers | computational chemistry | mechanism

The chemical depolymerization of common industrial plastics has recently attracted significant interest as an approach to mitigating environmental waste (1–4). To identify new roles for waste materials, new and inexpensive processes must be developed using polymers as starting materials. Research effort has been expended toward this end for the recycling of poly(ethylene terephthalate) (2, 3, 5), the polycondensation of end-capped poly(aryl ether sulfone) (PSU) for the in situ growth of poly(butylene terephthalate) block polymers (6), and the depolymerization of elemental sulfur for the synthesis of new polymeric materials (i.e., inverse vulcanization) (7). Notably, a complete bottle to bottle process has been developed to recycle poly(ethylene terephthalate) by chemical means (8). Not only has closed loop recycling been the goal of efforts such as these, but progress has also been made toward the depolymerization of waste materials into monomers for the ultimate formation of high-value polymeric materials. Such efforts have largely focused on the conversion of polymers into closely related derivatives—for example, the conversion of poly(ester)s into poly(amide)s (9) or poly(urethane) recycling by dynamic transcarbamoylation (10).

Herein, we describe a radically different approach to the repurposing of materials in which poly(carbonate)s (PCs) have been converted into PSUs in a single-step, single-vessel process. PCs are impact-resistant, optically clear thermoplastics used in industry for compact disks/DVDs, safety glass lenses, cockpit canopies, smartphones, and LCD screens, and they are the polymer of choice for automotive headlamp lenses (11). PCs are not typically recycled through conventional methods, because they do not have a unique resin identification code and therefore, fall into the “other” category

for plastics (12); as such, tons of PC waste often end up in landfills after use (11, 13).

We have taken advantage of the inherent decomposability of PCs in alkaline conditions to generate the bisphenol monomer, which is poised for additional reactivity in situ (Fig. 1). The principal challenges for polycondensation in a one-pot strategy are that (i) the depolymerization step goes to complete conversion, (ii) there are no side reactions, (iii) reagents remain pure during both steps, and (iv) the reactants are in perfect stoichiometric ratio to obtain respectable molecular masses. In addition, a one-pot approach to PSU synthesis negates the need for isolation or purification of intermediates, thus allowing direct access to PSU products and minimization of waste.

## Results and Discussion

**Polymer Formation.** We report a procedurally simple cascade reaction sequence involving depolymerization followed by polycondensation for the in situ synthesis of value-added, engineering thermoplastics. PCs were depolymerized and converted into PSUs in a single step. PSUs are high- $T_g$ , high-performance thermoplastics traditionally formed by the conversion of bisphenols into more reactive metal phenoxides (or other surrogates) that undergo  $S_NAr$  condensation with aryl fluorides proceeding through Meisenheimer intermediates (14, 15). Thus, poly(aryl ether sulfone)s have been produced from the reactions of aryl halides with bisphenols in the presence of stoichiometric amounts of metallic bases, or with silyl-protected bisphenols in the presence of metallic fluoride catalysts or organocatalysts (Fig. 1A) (15–17). Our approach involves the in situ generation of phenoxides from depolymerized poly(carbonate) waste and conversion of these intermediates into poly(aryl ether sulfone)s (Fig. 1B).

## Significance

This work describes a convenient, quantitative, and robust one-step transformation of polycarbonates into high-value poly(aryl ether sulfone)s in the presence of a carbonate salt and bis(aryl fluorides). This strategy has important implications for the repurposing of plastic waste into value-added materials by the use of carefully controlled depolymerization conditions. Computational studies used to support these findings show how carbonate salts decompose organic carbonates and form the poly(aryl ether sulfone) products. Determining the role of the metal salt in the depolymerization/repolymerization process will enable future design for economic recycling and synthesis methods.

Author contributions: J.L.H. and J.M.G. designed research; G.O.J., A.Y., R.J.W., and J.M.G. performed research; G.O.J., J.L.H., and J.M.G. analyzed data; and G.O.J. and J.M.G. wrote the paper.

The authors declare no conflict of interest.

This article is a PNAS Direct Submission. M.A.G.-G. is a guest editor invited by the Editorial Board.

<sup>1</sup>To whom correspondence may be addressed. Email: gojones@us.ibm.com or jmgarcia@us.ibm.com.

This article contains supporting information online at [www.pnas.org/lookup/suppl/doi:10.1073/pnas.1600924113/-DCSupplemental](http://www.pnas.org/lookup/suppl/doi:10.1073/pnas.1600924113/-DCSupplemental).

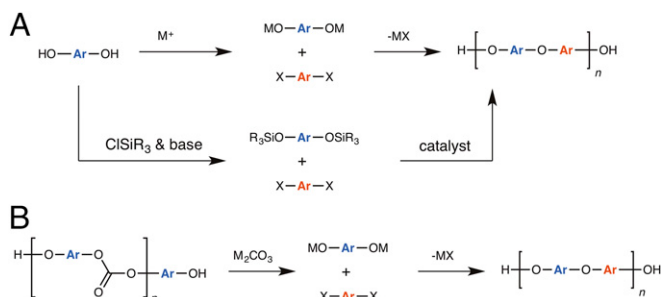


**Fig. 1.** (A) General approaches for poly(aryl ether) formation. (B) Our approach to poly(aryl ether) formation via the repurposing of poly(carbonate)s.

The depolymerization of poly[bisphenol A (BPA) carbonate] to liberate phenolic end groups and subsequent electrophilic trapping with 4,4'-difluorodiphenylsulfone allowed access to PSU in a one-step procedure, with loss of carbon dioxide as the byproduct. The depolymerization of PC to PSU proceeds cleanly (<sup>1</sup>H NMR spectra in Fig. 2, *Inset*) in this timeframe and produces a polymer with a single  $T_g$  and molecular mass comparable with starting material [gel permeation chromatography (GPC) traces are shown in Fig. 2 and the *SI Appendix*]. Notably, the  $T_g$  of PSU is  $\sim 30^\circ\text{C}$  higher than that of PC [ $T_g(\text{PC}) \sim 151^\circ\text{C}$ ;  $T_g(\text{PSU}) \sim 180^\circ\text{C}$ ]. This approach uses a cascade reaction involving the depolymerization of PC by  $\text{K}_2\text{CO}_3$  and formation of reactive phenoxides, which are then polycondensed in situ with 4,4'-difluorodiphenylsulfone. The reaction is complete within 18 h at  $190^\circ\text{C}$  in *N*-cyclohexyl-2-pyrrolidone. Crucially, the stringent requirements for step growth polymerizations are met under these conditions, which is a surprising and unexpected result; from a mechanistic standpoint, this transformation represents the first example, to our knowledge, of a macromolecule that is used as a monomer source for polycondensation.

Under the same conditions but when the monomer BPA is used instead of the polymer PC, the  $M_n$  (number average molar mass) of the isolated PSU is  $\sim 42.5$  kDa, which suggests that the kinetics of the reaction with PC is slower, which is to be expected given that PC must be depolymerized before polycondensation. The relative ratio of free OH end groups to F was  $\sim 1:2.6$ ,

consistent with observations for slow polycondensations that are subject to backbiting and formation of cyclic PSU side products during the polymerization (17). When the scale of the polymerization was increased, the average molecular mass increased by  $\sim 3$  kDa (Table 1), likely because of improvement in massing accuracy during experimental setup. To rule out effects from differences in retention volumes on molecular mass when measured against polystyrene standards, the PC starting material and PSU product were analyzed by GPC coupled with a light scattering detector. The PSU produced by this method had  $M_n = 27$  kDa, whereas the commercial PC starting material had an  $M_n = 20$  kDa (18).

The crude reaction mixture was analyzed after first depolymerizing PC with 1 eq  $\text{K}_2\text{CO}_3$  at  $190^\circ\text{C}$  for 18 h followed by addition of 4,4'-difluorodiphenylsulfone in *N*-methyl pyrrolidone (NMP) and continued heating for an additional 18 h. PSU oligomers were formed in low molecular masses ( $\sim 1$  kDa and below); however, 4,4'-difluorodiphenylsulfone was completely consumed (details in *SI Appendix*). We attribute the low molecular masses observed in this regime to the decomposition of solvent, which hampers the kinetics of polycondensation. In addition, when PC was heated in the absence of the aryl fluoride and the carbonate salt, no observable changes in PC signals were observed by <sup>1</sup>H NMR analysis on the sample in *d*<sub>6</sub>-DMSO within 3.5 h of heating at  $185^\circ\text{C}$  (details in *SI Appendix*), which suggests that the carbonate salt is required for PC decomposition. However, on the addition of  $\text{Li}_2\text{CO}_3$  (which exhibits some solubility in DMSO), <sup>1</sup>H NMR signals corresponding to BPA ( $\sim 6.7$  and  $7.0$  ppm) were observed within 40 min of heating ( $\sim 5\%$  conversion), and nearly complete depolymerization to BPA was observed after 19.5 h ( $\sim 88\%$  conversion) (Fig. 3). In addition to depolymerization of PC by carbonate salts, fluoride decomposition was also possible. When PC was treated with LiF, PC was depolymerized to a mixture of oligomers and BPA within the experimental timeframe (details in *SI Appendix*), suggesting that fluoride salts, the elimination byproduct of the  $\text{S}_{\text{N}}\text{Ar}$  step, are capable of depolymerizing PC. We hypothesize that PC decomposition by fluoride is caused by nucleophilic attack of fluoride on carbonate, leading to formation of carbonofluoric acid and carbonofluoric ester intermediates that can, in turn, react with water or hydroxide to form gaseous  $\text{CO}_2$  (details in *SI Appendix*).

These results prompted us to use substoichiometric quantities of  $\text{K}_2\text{CO}_3$  as an initiator given the ability of the LiF byproduct to also depolymerize PC. Thus, the depolymerization/polycondensation

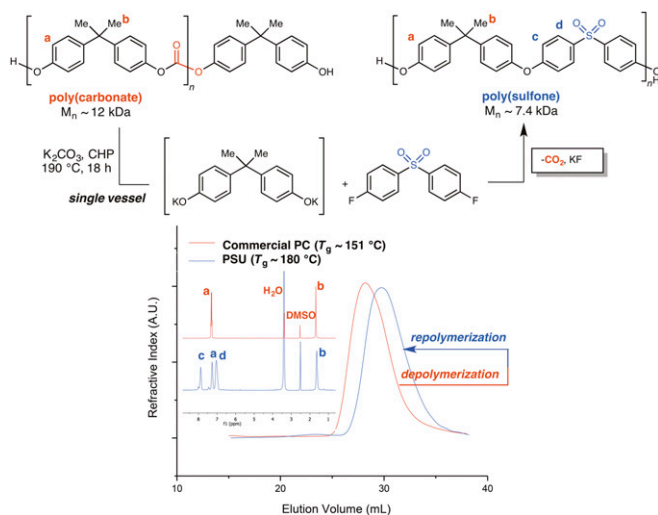


**Fig. 2.** GPC traces for PC (red) before in situ depolymerization by  $\text{K}_2\text{CO}_3$  in the presence of 4,4'-sulfonylbis(fluorobenzene) and PSU (blue) after reaction completion. (*Inset*) <sup>1</sup>H NMR of PC before depolymerization (upper trace) and PSU after repolymerization (lower trace). CHP, *N*-cyclohexyl-2-pyrrolidone.

**Table 1. Comparison of PSU molecular masses in varying conditions**

Entry	Conditions	$M_w$ (kDa)*	$M_n$ (kDa)*	PDI*
1	1 eq PC, 1.05 eq $\text{Li}_2\text{CO}_3$ , 1 eq ArF	19	11	1.82
2	1 eq PC, 1.05 eq $\text{K}_2\text{CO}_3$ , 1 eq ArF	16; 30 <sup>†</sup>	7.4; 27 <sup>†</sup>	2.09; 1.13 <sup>†</sup>
3	1 eq PC, 1.05 eq $\text{K}_2\text{CO}_3$ (18 h), 1 eq ArF (18 h)	<1	<1	ND
4	1 eq PC, 1.05 eq $\text{K}_2\text{CO}_3$ , 1 eq ArF (multigram scale)	20	10	1.94
5	1 eq BPA, 1.05 eq $\text{K}_2\text{CO}_3$ , 1 eq ArF	70	43	1.63
6	1 eq PC, 3.6 eq $\text{K}_2\text{CO}_3$ , 1 eq ArF	4.5	2.6	1.73
7	1 eq CD pieces, 1 eq $\text{K}_2\text{CO}_3$ , 1 eq ArF	20	11	1.73

ArF, 4,4'-difluorodiphenylsulfone; CD, compact disk;  $M_w$ , molecular weight; ND, not determined; PDI, polydispersity index.

\*Measured by GPC against polystyrene standards.

<sup>†</sup>Absolute molecular mass measured by GPC coupled with a light scattering detector; differential index of refraction,  $\text{dn}/\text{dc}$  (PSU) =  $0.156$  [ $M_w$  (PC) =  $23$  kDa;  $M_n$  (PC) =  $20$  kDa; PDI =  $1.16$ ;  $\text{dn}/\text{dc}$  (PC) =  $0.186$ ].

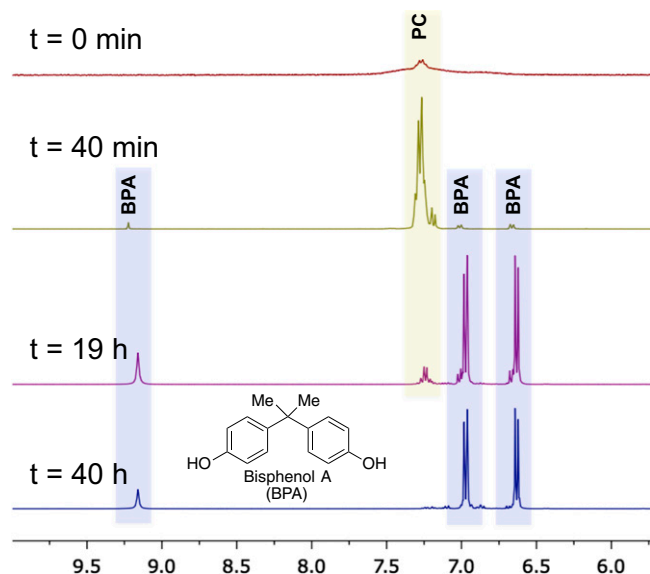


**Fig. 3.**  $^1\text{H}$  NMR study of depolymerization of PC by stoichiometric  $\text{Li}_2\text{CO}_3$  ( $d_6$ -DMSO; 185  $^\circ\text{C}$ ).

reaction was attempted with catalytic  $\text{K}_2\text{CO}_3$  (12 mol %). Under catalytic conditions,  $\sim 30\%$  of 4,4'-difluorosulfone reacted to form ether linkages within 24 h, which is unsurprising given that two phenoxide end groups are formed on cleavage of the carbonate linker (vide infra) (details in *SI Appendix*). Fewer than 2% of the signals corresponded to phenoxides derived from unreacted BPA or PC oligomers, indicating that ether formation is dependent on the initial depolymerization of PC and that phenoxide-terminated products, which may be oligomeric, are instantly consumed through  $\text{S}_{\text{N}}\text{Ar}$  with the aryl fluoride. Although PSU signals were not detected under these conditions, multiple signals characteristic of gem-dimethyl groups were observed by  $^1\text{H}$  NMR. Differential scanning calorimetry analysis on the product, which showed a single  $T_g$  at  $\sim 100$   $^\circ\text{C}$ , suggested that PC decomposition was incomplete and formed miscible oligomers with varied molecular masses that react with the aryl fluoride. Furthermore, the molecular mass of the product was diminished from the initial molecular mass of PC ( $M_n$  decreased from  $\sim 12$  to  $\sim 4$  kDa by GPC) (details in *SI Appendix*). The isolation of this intermediate suggests that the reaction of PC oligomers with 4,4'-difluorodiphenylsulfone was kinetically favored over depolymerization and that PSU formed after repeated depolymerizations and condensations over 18 h.

It is noteworthy that, in this reaction,  $\text{K}_2\text{CO}_3$  not only depolymerizes PC but is also itself degraded by the depolymerization process and serves as a catalyst for polyether formation in the subsequent step. To

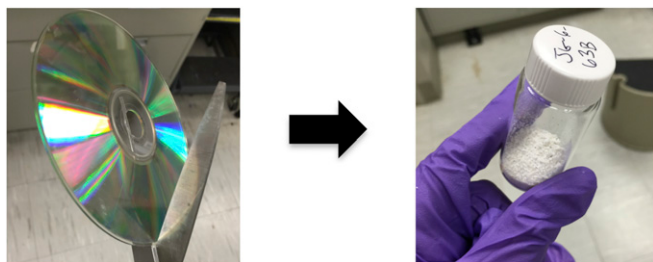


**Fig. 4.** Repurposing a compact disk as a monomer source for the depolymerization of PC and repolymerization to PSU. Compact disk (left) and PSU powder (right) are shown before and after the depolymerization/repolymerization process.

our knowledge, the methodology presented herein represents the first example of complete conversion of a step growth polymer into a dissimilar step growth polymer through in situ polymerization.

Finally, to assess the ability to transform materials comprised of PC into PSU with this method, a compact disk was exposed to the depolymerization/repolymerization reaction conditions in the presence of the aryl fluoride and  $\text{K}_2\text{CO}_3$  (Fig. 4). Conversion to PSU in this fashion was equally as efficient and produced polymers with comparable molecular masses as when purified PC pellets were used as starting materials [ $M_n$  (PSU)  $\sim 11$  kDa]. We envision that this method could also be applied to baby bottles formulated from poly(BPA carbonate) or other materials in a one-pot fashion.

**Computational Results.** Computational investigations were performed di-*p*-tolyl carbonate (PTC) and 1-fluoro-4-(methylsulfonyl)benzene (FSB) as computational models for PC and the bis(aryl fluoride) used in experiments, respectively (Fig. 5). The model reaction requires the use of 1 eq each PTC and sodium carbonate and 2 eq FSB and results in the formation of 2 eq each ether, gaseous  $\text{CO}_2$ , and sodium fluoride. These investigations involved the use of B3LYP-D3/ aug-cc-pVTZ//6-311+G(2d,p) (19–26) in implicit DMA solvent with the solvation model based on density (SMD) (27) to determine the mechanism and energetics for the depolymerization of PC by  $\text{Na}_2\text{CO}_3$  and subsequent polyether formation (Figs. 6 and 7 and details in *SI Appendix*).

The mechanism begins with the formation of intermediate 1 (INT1), a complex that is 23 kcal/mol more stable than the reactants on the free energy surface and comprises  $\text{Na}_2\text{CO}_3$  coordinated to PTC through a very favorable interaction between the sodium atoms of  $\text{Na}_2\text{CO}_3$  and the oxygen atoms of the organic carbonate. The free energy barrier for nucleophilic attack by  $\text{Na}_2\text{CO}_3$  on PTC in transition state 1 (TS1) is 17 kcal/mol with respect to INT1. TS1 leads to the formation of an oxodimethoxy carbonate intermediate, INT2, with a tetrahedral carbon attached to four oxygen atoms.

INT2 is energetically unstable, is in a shallow minimum, and quickly decomposes to INT3; TS2, the transition state for the decomposition of INT2, possesses a free energy barrier of only  $\sim 5$  kcal/mol with respect to INT2 ( $\sim 20$  kcal/mol with respect to INT1). Two concomitant processes occur in TS2: breakage of the C–O4 bond, which leads to  $\text{CO}_2$  formation, and breakage of the C5–O6 bond, which converts the tetrahedral  $\text{C}(\text{sp}^3)$ –O4 into a trigonal  $\text{C}(\text{sp}^2)$ –O3 (Fig. 6). The intermediate resulting from  $\text{CO}_2$  formation, INT3, is  $\sim 47$  kcal/mol more stable than the reactants; it comprises a covalently bonded disodium complexed to the  $\text{CO}_2$  molecule, cresolate, and PTC.

Dissociation of  $\text{CO}_2$  from INT3 results in the formation of INT4, which is  $\sim 11$  kcal/mol more stable than INT3. The exergonicity for  $\text{CO}_2$  dissociation from INT3 is likely caused by the entropy gained by dissociation of the gaseous  $\text{CO}_2$  molecule from the solvated complex. The second molecule of  $\text{CO}_2$  is formed from INT4 in TS3 and results in the formation of INT5, in which the sodium cresolate dimer is bound to the  $\text{CO}_2$  molecule. TS3 possesses a free energy barrier of  $\sim 26$  kcal/mol with respect to INT4, and INT5 is  $\sim 21$  kcal/mol less stable than INT4. Formation of the second molecule of  $\text{CO}_2$  from the second molecule is notably less favorable than formation of the first molecule, presumably because the first molecule of  $\text{CO}_2$  is formed from an energetically unstable oxodimethoxy carbonate comprising a tetrahedral carbon atom bonded to four oxygen atoms in INT2. By contrast, the second molecule of  $\text{CO}_2$  is formed from a comparatively more stable ionic

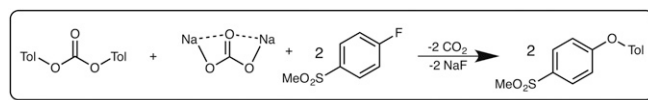


**Fig. 5.** Computational models for ether formation from the reaction of PTC with FSB in the presence of  $\text{Na}_2\text{CO}_3$ .

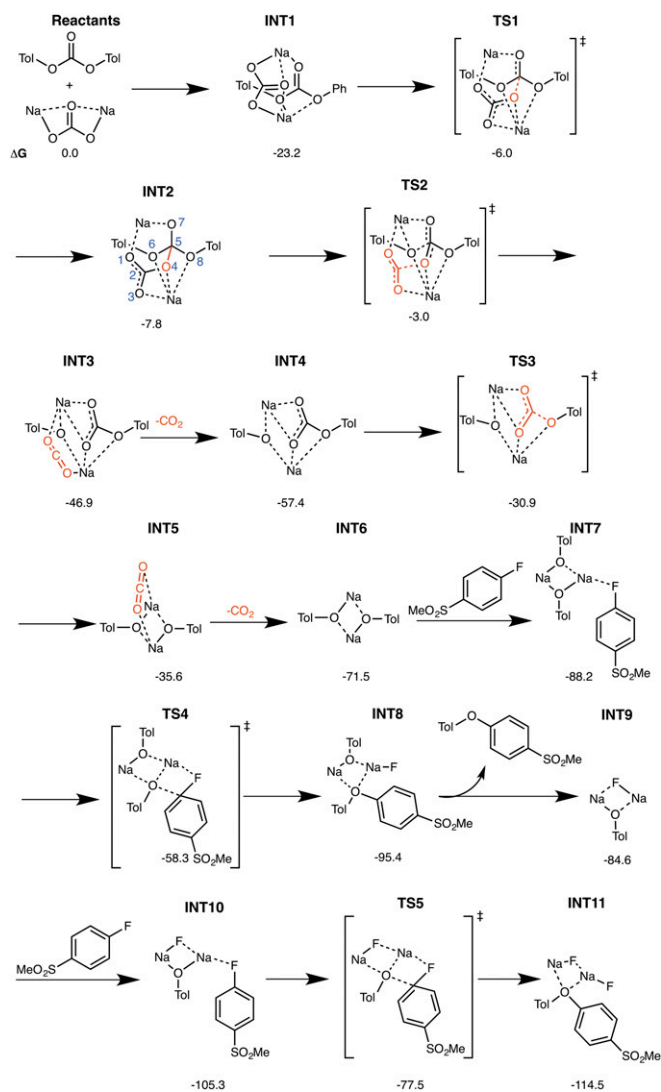


**Fig. 6.** Stationary points and free energies for ether formation from the reaction of PTC with FSB in the presence of  $\text{Na}_2\text{CO}_3$ .

carbonate, which is less likely to release carbon dioxide. Dissociation of the second molecule of  $\text{CO}_2$  from INT5 results in the exergonic formation of the sodium cresolate dimer, INT6, which is  $\sim 36$  kcal/mol more stable than INT5 ( $\sim 24$  kcal/mol below INT4). As before, this observed exergonicity is likely caused by the entropy gain from gaseous  $\text{CO}_2$  dissociation from the solvated complex.

We next considered whether formation of the initial ether molecule proceeds directly from the sodium cresolate dimer, INT6 (i.e., whether the dimer dissociates and forms sodium cresolate before reacting with an aryl fluoride present in the reaction or whether INT6 is directly involved in ether formation). The former scenario could be ruled out because of the fact that formation of two molecules of sodium cresolate from INT6 is endergonic (41 kcal/mol above INT6), presumably because of the presence of the strong disodium bond. In contrast, formation of INT7 by the coordination of the sodium cresolate dimer with FSB is exergonic by about 17 kcal/mol with respect to INT6. The transition state for ether formation proceeding directly from the covalently bound sodium cresolate dimer, TS4, possesses a free energy barrier of  $\sim 30$  kcal/mol with respect to INT7 and forms INT8, in which the ether is bound to a datively coordinated sodium fluoride–sodium cresolate complex. Dissociation of ether from INT8 is endergonic

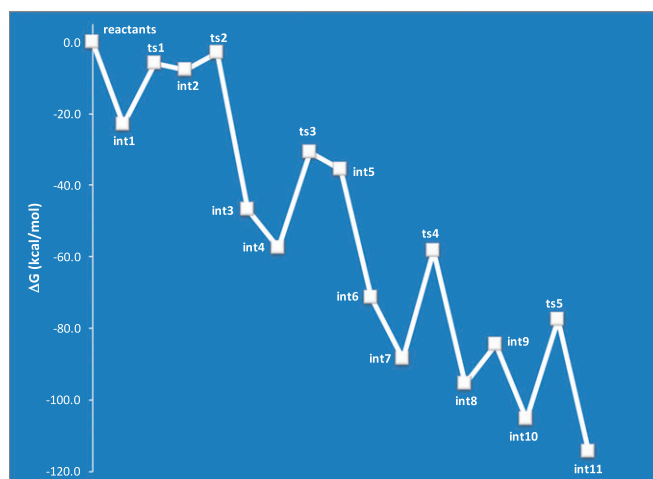


**Fig. 7.** Free energy surface for ether formation from the reaction of PTC with FSB in the presence of  $\text{Na}_2\text{CO}_3$ .

by about 10 kcal/mol owing to the favorable binding of sodium with oxygen; dissociation leads to the formation of INT9, a datively coordinated sodium fluoride–sodium cresolate complex. Coordination of the second molecule of FSB to INT9 produces INT10, which is  $\sim 21$  kcal/mol more stable than INT9. Notably, there is a net free energy gain after an incoming FSB molecule coordinates to the sodium fluoride–sodium cresolate complex formed after ether dissociation; this free energy gain mitigates the fact that ether dissociation from the sodium fluoride–sodium cresolate complex is an endergonic process.

The second ether molecule is formed from INT10, which proceeds through TS5 to produce INT11, a complex comprising the ether molecule bound to two molecules of sodium fluoride. The free energy barrier for formation of the second ether molecule in TS5 is  $\sim 28$  kcal/mol with respect to INT10. The release of the second ether molecule from INT11 is expected to be slightly endergonic (similar to the release of the first ether molecule from INT8 to form INT9) because of the favorable binding of sodium to the oxygen belonging to the ether, but in general, the free energy profile is exergonic starting from the reactants.

Overall, these calculations signify that the decomposition of organic carbonates by carbonate salts into phenolate dimers is a facile process. In addition, these phenolate dimers are competent substrates for ether formation from reactions involving aryl fluorides.

In conclusion, we have shown formation of high-value PSUs from the in situ depolymerization of PCs in a single operation in the presence of a carbonate salt and bis(aryl fluoride)s. This strategy has important implications for the formation of value-added polymeric materials from plastic waste (for example, recycling). Given the stringent criteria for step growth polymerization, including the absence of side reactions, perfect stoichiometry, and quantitative conversion of monomer to polymer, the PSU formation shown herein attests to the robustness of the depolymerization and repolymerization process. Computational studies used to support these findings show that carbonate salts decompose organic carbonates through initial nucleophilic attack followed by the loss of  $\text{CO}_2$  and formation of phenoxide dimers and subsequently, ether products. We envision that careful control over depolymerization reactions to form materials by coupling computation with experiments will ultimately enable repurposing of spent polymeric materials.

## Materials and Methods

Full materials and methods are provided in *SI Appendix*.

**ACKNOWLEDGMENTS.** We thank Teddie Magbitang for assistance with light scattering GPC analysis and Andy Tek for thermal analysis.

1. Aguado J, Serrano DP (1999) *Feedstock Recycling of Plastic Wastes* (Royal Society of Chemistry, Cambridge, UK).
2. Nikles DE, Farahat MS (2005) New motivation for the depolymerization products derived from poly(ethylene terephthalate) (PET) waste: A review. *Macromol Mater Eng* 290(1):13–30.
3. Sinha V, Patel MR, Patel JV (2010) PET waste management by chemical recycling: A review. *J Polym Environ* 18(1):8–25.
4. Achilias D, ed (2012) *Material Recycling - Trends and Perspectives*. (InTech, Rijeka, Croatia). Available at [www.intechopen.com/books/material-recycling-trends-and-perspectives](http://www.intechopen.com/books/material-recycling-trends-and-perspectives). Accessed November 18, 2015.
5. Bartolome L, Imran M, Gyoo BAW, Hyun D (2012) Recent developments in the chemical recycling of PET. *Material Recycling - Trends and Perspectives*, ed Achilias DS (InTech, Rijeka, Croatia). Available at [www.intechopen.com/books/material-recycling-trends-and-perspectives/recent-developments-in-the-chemical-recycling-of-pet](http://www.intechopen.com/books/material-recycling-trends-and-perspectives/recent-developments-in-the-chemical-recycling-of-pet). Accessed November 18, 2015.
6. Dennis JM, Fahs GB, Moore RB, Turner SR, Long TE (2014) Synthesis and characterization of polysulfone-containing poly(butylene terephthalate) segmented block copolymers. *Macromolecules* 47(23):8171–8177.
7. Chung WJ, et al. (2013) The use of elemental sulfur as an alternative feedstock for polymeric materials. *Nat Chem* 5(6):518–524.
8. Fukushima K, et al. (2011) Organocatalytic depolymerization of poly(ethylene terephthalate). *J Polym Sci A Polym Chem* 49(5):1273–1281.
9. Fukushima K, et al. (2013) Advanced chemical recycling of poly(ethylene terephthalate) through organocatalytic aminolysis. *Polym Chem* 4(5):1610–1616.
10. Fortman DJ, Brutman JP, Cramer CJ, Hillmyer MA, Dichtel WR (2015) Mechanically activated, catalyst-free polyhydroxyurethane vitrimers. *J Am Chem Soc* 137(44):14019–14022.
11. Antonakou EV, Achilias DS (2013) Recent advances in polycarbonate recycling: A review of degradation methods and their mechanisms. *Waste Biomass Valorization* 4(1):9–21.
12. ASTM International (2013) *ASTM D7611 - Standard Practice for Coding Plastic Manufactured Articles for Resin Identification* (ASTM International, West Conshohocken, PA).
13. Vogel SA (2009) The politics of plastics: The making and unmaking of bisphenol a "safety." *Am J Public Health* 99(Suppl 3):S559–S566.
14. El-Hibri MJ, Nazabal J, Eguizabal JI, Arzak A (1997) Poly(aryl ether sulfone)s. *Handbook of Thermoplastics*, eds Olabisi O, Adewale K (CRC Press, Boca Raton, FL), pp 893–930.
15. Labadie JW, Hedrick JL, Ueda M (1996) Poly(aryl ether) synthesis. *Step-Growth Polymers for High-Performance Materials*, ACS Symposium Series, eds Hedrick JL, Labadie JW (American Chemical Society Washington, DC), pp 210–225.
16. Olabisi O, Adewale K, eds. (1997) *Handbook of Thermoplastics* (CRC Press, Boca Raton, FL).
17. Garcia JM, et al. (2014) Meisenheimer complex inspired catalyst- and solvent-free synthesis of noncyclic poly(aryl ether sulfone)s. *Macromolecules* 47(23):8131–8136.
18. Ioan S, Filimon A, Avram E (2005) Influence of degree of substitution to the optical properties of chloromethylated polysulfone. *J Macromol Sci Part B* 44(1):129–135.
19. Becke AD (1993) Density-functional thermochemistry. III. The role of exact exchange. *J Chem Phys* 98(7):5648–5652.
20. Lee C, Yang W, Parr RG (1988) Development of the Colle-Salvetti correlation-energy formula into a functional of the electron density. *Phys Rev B Condens Matter* 37(2):785–789.
21. Vosko SH, Wilk L, Nusair M (1980) Accurate spin-dependent electron liquid correlation energies for local spin density calculations: A critical analysis. *Can J Phys* 58(8):1200–1211.
22. Stephens PJ, Devlin FJ, Chabalowski CF, Frisch MJ (1994) Ab initio calculation of vibrational absorption and circular dichroism spectra using density functional force fields. *J Phys Chem* 98(45):11623–11627.
23. Grimme S, Antony J, Ehrlich S, Krieg H (2010) A consistent and accurate ab initio parametrization of density functional dispersion correction (DFT-D) for the 94 elements H-Pu. *J Chem Phys* 132(15):154104–154119.
24. Woon DE, Dunning TH (1995) Gaussian basis sets for use in correlated molecular calculations. V. Core-valence basis sets for boron through neon. *J Chem Phys* 103(11):4572–4585.
25. Kendall RA, Dunning TH, Harrison RJ (1992) Electron affinities of the first-row atoms revisited. Systematic basis sets and wave functions. *J Chem Phys* 96(9):6796–6806.
26. Krishnan R, Binkley JS, Seeger R, Pople JA (1980) Self-consistent molecular orbital methods. XX. A basis set for correlated wave functions. *J Chem Phys* 72(1):650–654.
27. Marenich AV, Cramer CJ, Truhlar DG (2009) Universal solvation model based on solute electron density and on a continuum model of the solvent defined by the bulk dielectric constant and atomic surface tensions. *J Phys Chem B* 113(18):6378–6396.